Interannual SST Variability in the Southern Subtropical and Extra-tropical Ocean

Bohua Huang[1,2] *and J. Shukla*[1,2]

[1]Department of Climate Dynamics
College of Science
George Mason University
Fairfax, Virginia

[2]Center for Ocean-Land-Atmosphere Studies
Institute of Global Environment and Society
4041 Powder Mill Road, #302
Calverton, Maryland 20705
huangb@cola.iges.org

October 2006

Abstract

The interannual variability of the sea surface temperature (SST) in the southern oceans shows an unrecognized ubiquitous feature. In contrast to their northern counterparts, active SST fluctuations occur in the open oceans in all three major basins, which are unattached to the coastal processes. Using historical SST observations for 1950-2000, it is shown that these extra-tropical/subtropical SST anomalies have a tilted southwest-northeast dipole pattern in both the Atlantic and Indian Oceans and, to a certain extent, in the central and eastern Pacific. SST fluctuations in all basins show similar seasonal enhancement in austral summer. A long-term simulation of a coupled ocean-atmosphere general circulation model reproduces some of these major features realistically, especially in the South Atlantic. A composite analysis of the objectively selected major events in the South Atlantic from the observations and the simulation shows that the anomalous SST pattern is initiated by mid-latitude atmospheric fluctuations. Through a coupled air-sea feedback, the center of the subtropical branch of the SST anomalies can shift towards the tropics in the next season.

1. Introduction

In the southern ocean, seasonal mean anomalies of the sea surface temperature (to be referred to as SSTA hereafter) usually appear in broad areas between 20ºS-50ºS, as shown by the local maxima of standard deviation at around 0.4º-0.6ºC in all three basins (Fig.1). These SSTAs taper off poleward, possibly because the formation and melting of sea ice limit the range of temperature change at neighboring water. Further to the north, the major areas of strong subtropical SSTA standard deviation (> 0.4ºC) are separate from those in the equatorial regions. This separation suggests that the subtropical SSTA is distinct from the dynamically generated SSTA in both the equatorial Atlantic and Pacific Oceans. It should be pointed out that the subtropical/extra-tropical SSTAs in the northern oceans, which are generally more intense than their southern counterparts, share these general features. A major difference between them, however, is that the southern SSTA usually appears within the open ocean detached from continents, while the northern SSTA is generally linked geographically to major fluctuations near the coasts, implying the contributions by either the upwelling near the eastern boundaries or the Gulf Stream and Kuroshio extensions in the west. The uniqueness of the SST anomalies in the southern subtropical and extra-tropical oceans deserves further analysis.

There have been some previous studies on the subtropical and extratropical SST fluctuations in individual basins of the Southern Ocean, especially the South Atlantic Ocean. Using observational datasets, Venegas et al. (1997) and Robertson and Mechoso (2000) respectively derived major SSTA patterns in the South Atlantic and analyzed their relationships with atmospheric fields. Examining the heat budget of the oceanic mixed layer, Sterl and Hazeleger (2003) found that the SSTAs in the South Atlantic are largely

forced by the atmospheric latent heat flux. Forcing an atmospheric general circulation model (AGCM), Robertson et al. (2003) showed that the prescribed SSTA in the subtropical South Atlantic generates an atmospheric baroclinic response near the South Atlantic convergence zone (SACZ). Through idealized SSTA forcing experiments, Reason and Jagadheesha (2005) also showed that the precipitation over the Southwestern Cape region of the South Africa is influenced by the large-scale atmospheric anomalies induced by the subtropical-mid-latitude SSTA during austral winter.

Using a coupled ocean-atmosphere GCM (CGCM), Huang and Shukla (2005) studied the air-sea interactions associated with the SSTA evolution in the subtropical South Atlantic Ocean. They found that the SSTA is generally initiated by extra-tropical atmospheric forcing. Once the SSTA is generated, it feeds back actively to the atmosphere and, through a coupled interaction, the air-sea anomalies expand toward the tropical and equatorial ocean. However, since this particular model was coupled within the Atlantic basin only to the north of 30ºS, the feedback was confined to the tropical-subtropical ocean.

In this study, we will demonstrate the common character of the subtropical-midlatitude SST variations in the three major basins of the Southern Ocean. The SSTA pattern in the South Atlantic Ocean will be used as an example to explain the SST fluctuations in the other two basins of the southern ocean, including the subtropical dipole SST mode in the South Indian Ocean (Behera and Yamagata 2001, Suzuki et al., 2004; Huang and Shukla 2006), which is distinct from the popular tropical dipole/zonal mode (e.g., Saji et al., 1999) but similar to the South Atlantic SSTA discussed above in some aspects. Accompanying the analysis of historical datasets, we will also examine a

long-term globally coupled GCM simulation, which expands the results from Huang and Shukla (2005) by including extra-tropical air-sea interactions. The data and model are described briefly in the next section and the results are presented in Section 3. A summary is given in Section 4.

2. Data and model

In this study, we use the improved extended reconstruction of the monthly mean global SST analysis (ERSST, version 2, Smith and Reynolds, 2004) for 1950-2000. The SST analysis is on a 2^{o} latitude x 2^{o} longitude grid, produced from the latest version of the Comprehensive Ocean-Atmosphere Data Set (COADS). The corresponding atmospheric monthly mean data for the same period are from the National Centers for Environment Predictions (NCEP) and National Center for Atmospheric Research (NCAR) meteorological reanalysis (Kalnay et al., 1996). The monthly anomalies are calculated from the climatological monthly means based on the 51-year record. These anomalies are then averaged to form seasonal means for December-February (DJF), March-May (MAM), June-August (JJA), and September-November (SON), which correspond to austral summer, fall, winter, and spring respectively. All seasonal data are detrended. In particular, this procedure eliminates a long-term tendency in the reanalyzed sea level pressure (SLP) fields. The existence of such a trend needs further validation because of the potentially large errors in the reanalyzed SLP in mid and high latitudes of the southern hemisphere (Kistler et al., 2001), which is beyond the scope of the present study.

The atmospheric component of the CGCM is a global spectral AGCM with a triangular truncation of the spherical harmonics at T42 (Schneider et al., 2001).

Vertically, it is divided into 18 σ levels with higher resolution in the lower troposphere. The model has the same dynamical core as that of the NCAR Community Climate Model (version 3.0). Its subscale physical parameterization is state-of-the-art. The oceanic GCM (OGCM) is a quasi-isopycnal model of 14 active layers (Schopf and Loughe, 1995). Its domain is the World Oceans within 70°S-65°N with a horizontal resolution of 1° latitude x 1.25° longitude while the meridional resolution is increased to 0.5° within 10°S-10°N. The 1st model layer represents the oceanic mixed layer with the entrainment at its base calculated following Niiler and Kraus (1977). The vertical mixing below the mixed layer is dependent on the Richardson number. The coupling between the OGCM and the AGCM is on a daily interval.

The globally coupled model is integrated for 500 years with initial conditions derived from long-term uncoupled simulations. The last 300-year simulation of the CGCM is used in this study. We found that the CGCM produces a realistic seasonal climatology of the surface wind stress, SST, and SLP in the southern ocean (not shown). A major shortcoming of the simulation is the larger amplitudes in the annual cycles of the model variables than is observed in the higher latitudes of the extratropical region. A possible reason is that the surface heat exchange with the atmosphere changes water temperature instead of producing or melting sea ice. The consequences can be clearly seen in the following discussions.

3. Results

We have calculated the leading modes of the empirical orthogonal functions (EOF) of the seasonally averaged SSTA from both the observations and the CGCM. All seasons are included in the calculation. The spatial domains of the EOF calculation are

chosen to cover the regions of large standard deviations in the open southern ocean, as shown by the rectangles in the three basins (Fig.1).

Figure 2 shows the 1st EOF modes of the SSTA in the South Atlantic Ocean for the observations and the CGCM. It can be seen that both the observations and the model show a dipole pattern with the positive center located at 20ºS and 10ºW-20ºW and the negative center around 35ºS-40ºS and 20ºW-30ºW. The positive node shows a clear southeastward tilt across the basin. This pattern is similar to those derived by previous observational studies in this region (e.g., Venegas et al., 1997; Sterl and Hezaleger 2003). As far as we know, the CGCM's capability to simulate this full pattern has not been demonstrated before. As we have pointed out earlier, Huang and Shukla's (2005) previous regional coupled simulation reproduced the SSTA associated with the positive node of this mode, which they named as the southern subtropical Atlantic (SSA) pattern.

A very similar pattern exists in the South Indian Ocean (Fig.3a), which gives a dipole pattern between an elongated positive region extending from the western Australian coast toward the central equatorial Indian Ocean and a negative center located near 40ºS-45ºS and 60ºE-70ºE. This mode explains about 22% of the total variance. Using a monthly SST dataset for 1958-98 on a different spatial domain, Behera and Yamagata (2001) derived a similar spatial pattern, which they named as the subtropical SST dipole pattern. The CGCM reproduces the basic features of this pattern (Fig.3b), including the locations of the major nodes, as well as the tilting of the northern one. However, there are major discrepancies between the model and the observations. Compared with the observations, the CGCM northern node is weak while its southern node is elongated zonally and its center is about 10º to the east of the observations.

Moreover, an opposite change occurs to the south of 45°S, which does not appear in the observations.

In the South Pacific, the domain of the EOF calculation is shifted southward to include the significant SSTA fluctuations there (Fig.1) and avoid the direct effects of the strong equatorial SST variability due to the El Niño/Southern Oscillation (ENSO). The result shows that the major SST mode is a seesaw between the subtropical and extra-tropical ocean (Fig.4a). In the northern part, there are two centers located near New Zealand and the central Pacific around 30°S. The structure of the latter is reminiscent of the northern node of the Atlantic mode (Fig.2a). The leading mode of the CGCM (Fig.4b) captures the major centers of the observed mode. However, the model spatial structure is much more zonal than the observed one, which is, to a certain degree, the situation in the South Indian Ocean also.

We have calculated the EOF modes using data for separate seasons. It is found that the EOF modes are quite strongly phase locked with the annual cycle. In general, these patterns are strongest in austral summer (DJF) and fall (MAM), and weakest in austral winter (JJA). This seasonal dependence is simulated quite well by the CGCM (not shown). Based on these results, it can be summarized that the relatively high SSTA standard deviation in the southern ocean is associated with dipole-like spatial structure of the SST anomalies from austral summer to fall.

To understand the mechanisms of these dipole-like patterns and their evolution, we have conducted composite analysis based on objectively selected major events peaking in austral summer. As an example, we present the composite results for the South Atlantic mode. A “major event” season is selected when it has a local maximum or

minimum of the principal component of the 1st DJF SSTA EOF, which is similar to those shown in Figs.2-4, and its amplitude is above one standard deviation. Based on this definition, 6 positive and 4 negative events are selected from the observations in 1950-2000. From the 300-yr CGCM run, 41 positive and 37 negative events are selected.

Figure 5 shows the evolution of the observed composite anomalous event from austral summer (DJF) to fall (MAM). In fact, this event can be traced back to the previous spring season (SON) when a seasonal anomalous low SLP center appears in 50°S and 20°W (not shown). By DJF, the SLP center has shifted slightly northeastward (Fig.5c). Associated with it, there is an anomalous surface cyclonic circulation over the South Atlantic (Fig.5a). In particular, anomalous northwesterly winds prevail over the subtropical ocean from 10°S to 30°S, which reduces the total trade winds and the surface heat loss through evaporation. As a result, local SST increases. In the southwest, however, surface heat loss is increased possibly because the anomalous southerly winds enhance the total wind speed and enhanced local Ekman pumping. The same wind anomalies also advect colder surface air northward. These factors also contribute to the cooling of the sea surface in the southwestern ocean and the formation of the observed dipole-like pattern (Sterl and Hezeleger 2003).

It is interesting to see that the subtropical SST anomalies, once induced, are able to generate noticeable atmospheric responses. This can be seen from the reduction of the SLP near 20°S and 20°W-30°W in MAM (Fig.5d) over the highest SSTA (Fig.5b). By this season, the extra-tropical SLP center has been decaying and does not pass the 95% significance level. Instead, the major significant area of the SLP anomalies is shifted to the tropical ocean. The center of the warm SST anomalies is also shifted northwestward

from 25ºS 10ºW in DJF (Fig.5a) to 20ºS, 20ºW in MAM (Fig.5b). This slow migration can be explained by a coupled feedback among SLP, wind-induced surface evaporation, and SST (WES, Xie and Philander 1994; Tourre and White 1997). Due to this coupled process, strong extra-tropical atmospheric anomalies in austral spring and summer are capable of influencing the southern tropical climate in austral summer and fall.

The model composite (Fig.6) reproduces these observational features realistically, including the initial mid-latitude atmospheric fluctuation, its generation of the dipole-like SSTA, and the modification of the tropical SLP and SST. Our composites of the upper atmospheric variables suggest that the atmospheric response is baroclinic, involving the heat sources associated with the disturbances of the SACZ (not shown), which is consistent with the uncoupled AGCM results by Robertson et al. (2003).

Our composites in the other two ocean basins follow a somewhat similar pattern. In general, they demonstrate that the dipole-like SSTA structures there are also responses to the mid-latitude atmospheric fluctuations. In the South Indian Ocean, our results are consistent with those by Behera and Yamagata (2001) and the CGCM model results by Suzuki et al. (2004). From observations, we found noticeable influences of the subtropical SSTA on the local SLP in the South Indian Ocean in a similar fashion as in the South Atlantic. In the CGCM, however, it is the southwestern node of the mode that influences the subsequent SST development significantly, as demonstrated by Huang and Shukla (2006), possibly because the CGCM northern node is too weak.

4. Summary and discussion

In this study, we have demonstrated the existence of a ubiquitous SST interannual variability in the southern oceans, which to our knowledge has not been reported before

as a general feature of the southern oceans. In particular, active SSTA fluctuations occur in the open ocean in the subtropical-mid-latitude region in all three major basins. Using historical observational datasets and a long-term CGCM simulation, we have demonstrated that these extra-tropical/subtropical SSTAs have a tilted southwest-northeast dipole pattern in both the Atlantic and Indian Oceans and, to a certain extent, in the central and eastern Pacific. Further composite analysis shows that this SSTA pattern is initiated by the oceanic response to mid-latitude atmospheric fluctuation. However, the subtropical branch of the forced SSTA can feedback to the atmosphere and induce a longer-term influence on the tropical climate.

This study demonstrates that the atmospheric internal variability in the mid-latitude may contribute to the predictability of the tropical climate on a seasonal scale. Even though the mid-latitude disturbance is not predictable itself, the chain of events initiated by this initial perturbation is predictable to a certain degree. Some more sophisticated procedures of model initialization are required to introduce these signals into the coupled forecast system.

There are multiple sources of mid-latitude atmospheric variability. One CGCM discrepancy from the observations in this respect is its overly strong southern annular mode. This is the major reason for the more zonal orientation of the SSTA spatial structure in both the Indian and the Pacific Oceans. We also found that the model SSTA in different basins show quite coherent patterns. Although the observed southern annular mode may have a similar influence on the southern ocean (e.g., Hermes and Reason 2005), it seems much weaker than that shown in the CGCM. We speculate that better sea ice treatment may improve the simulation in the southern ocean significantly.

Acknowledgments

The financial support of this study is provided by a joint grant from NSF, NOAA, and NASA (NSF 0332910, NOAA NA04OAR4310034 and NASA NNG04GG46G). Huang is also supported by a grant from NOAA's CLIVAR Atlantic Program (NA04OAR4310115). We thank Drs. D. Straus and S. Bates for carefully reading the manuscript and constructive comments.

References

Behera, S. K., T. Yamagata, 2001: Subtropical SST dipole events in the southern Indian Ocean, *Geophys. Res. Lett.*, **28**, 327-330, 10.1029/2000GL011451.

Hermes, J.C., and C.J.C. Reason, 2005: Ocean model diagnosis of interannual coevolving SST Variability in the South Indian and South Atlantic Oceans. *J. Climate*, **18**, 2864–2882.

Huang, B., and J. Shukla, 2006: On the mechanisms for the interannual variability in the tropical Indian Ocean. Part II: Regional processes. *J. Climate*, in press.

Huang, B., and J. Shukla, 2005: The ocean-atmospheric interactions in the tropical and subtropical Atlantic Ocean. *J. Climate*, **18**, 1652-1672.

Kalnay, E., co-authors, 1996: The NCEP-NCAR 40 year reanalysis project. *Bull. Amer. Meter. Soc.*, **77**, 437-471.

Kistler, R., and co-authors, 2001: The NCEP–NCAR 50–Year reanalysis: monthly means CD–ROM and documentation. *Bull. Amer. Meteor. Soc.,* **82**, 247-267.

Niiler, P.P., and E.B. Kraus, 1977: One-dimensional models of the upper ocean. *Modelling and Prediction of the Upper Layers of the Ocean*. E.B. Kraus, Ed., Pergamon, 143-172.

Reason, C.J.C., and D. Jagadheesha, 2005: Relationships between South Atlantic SST variability and atmospheric circulation over the South African region during austral winter. *J. Climate*, **18**, 3339–3355.

Robertson, A.W., J.D. Farrara and C.R. Mechoso, 2003: Simulations of the atmospheric response to South Atlantic sea surface temperature anomalies. *J. Climate*, **16**, 2540–2551.

Robertson, A.W., and C.R. Mechoso. 2000: Interannual and interdecadal Variability of the South Atlantic Convergence Zone. *Mon. Wea. Rev*., **128**, 2947–2957.

Saji, N.H., B.N. Goswami, P.N. Vinayachandran, and T. Yamagata, 1999: A dipole mode in the tropical Indian Ocean. *Nature*, **401**, 360-363.

Schneider, E.K., B.P. Kirtman, Y, Fan, and Z. Zhu, 2001: Retrospective ENSO forecasts: The effect of ocean resolution. *COLA Tech. Report*, **109**, 27pp.

Schopf, P. S., and, A. Loughe, 1995: A reduced gravity isopycnal ocean model: Hindcasts of El Niño. *Mon. Wea. Rev.,* **123**, 2839-2863.

Smith, T.M., and R.W. Reynolds, 2004: Improved Extended Reconstruction of SST (1854–1997). *J. Climate*, **17**, 2466–2477.

Sterl, A., and W. Hazeleger, 2003: Coupled variability and air-sea interaction in the South Atlantic Ocean. *Clim., Dyn*., **21**, 559-571.

Suzuki, R., S.K. Behera, S. Iizuka, T. Yamagata, 2004: Indian Ocean subtropical dipole simulated using a coupled general circulation model. *J. Geophy. Res*., **109**, doi:10.1029/2003JC001974.

Tourre, Y.M., and W.B. White, 1997: Evolution of the ENSO signal over the Indo-Pacific domain. *J. Phys. Oceanogr*., **27**, 683-696.

Venegas, S.A., L.A. Mysak, and D.N. Straub. 1997: Atmosphere–ocean coupled variability in the South Atlantic. *J. Climate*, **10**, 2904–2920.

Xie, S.-P., and S.G.H. Philander, 1994: A coupled ocean-atmospheric model of relevance to the ITCZ in the eastern Pacific. *Tellus*, **46A**, 340-350.

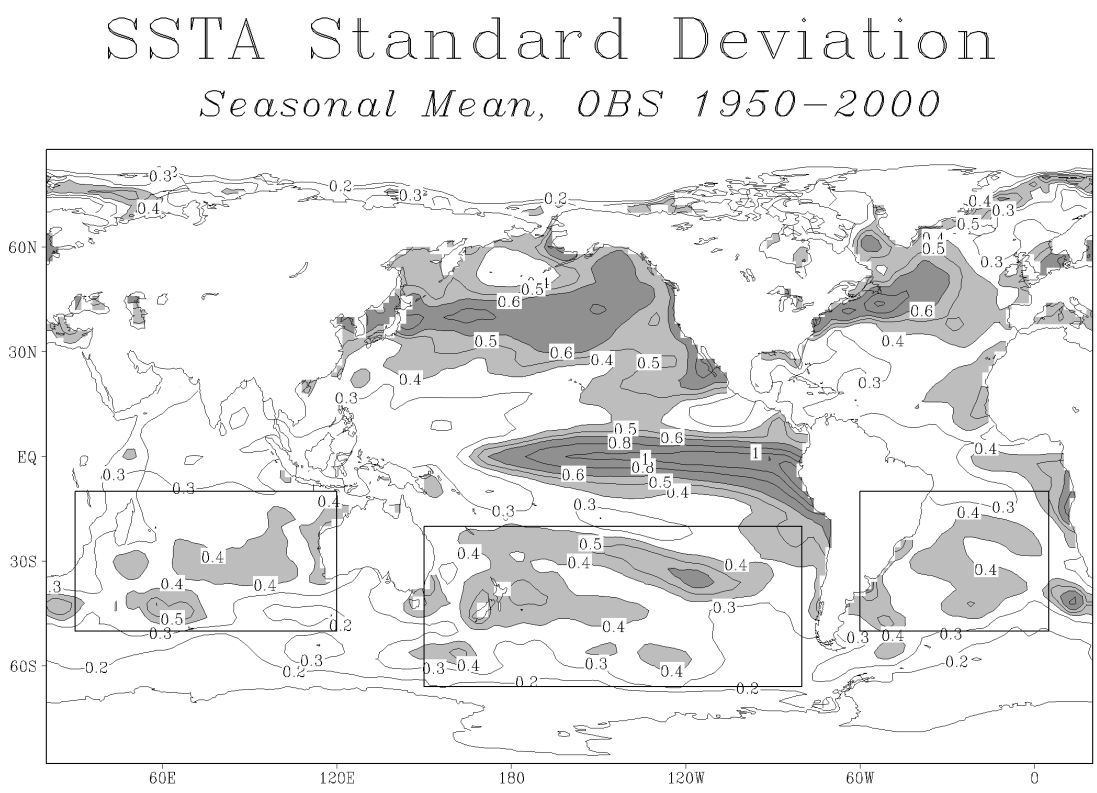

Figure 1 The standard deviation of the seasonally averaged observational SSTA for 1950-1998. The contour interval is 0.1ºC if the standard deviation is within the range of 0.2ºC-0.6ºC and 0.2ºC if it is above 0.6ºC. Values below 0.2ºC are not shown. The areas with standard deviation within 0.4ºC-0.6ºC are lightly shaded and those above 0.6ºC are darkly shaded. The rectangles identify the areas chosen for EOF analysis in the three ocean basins.

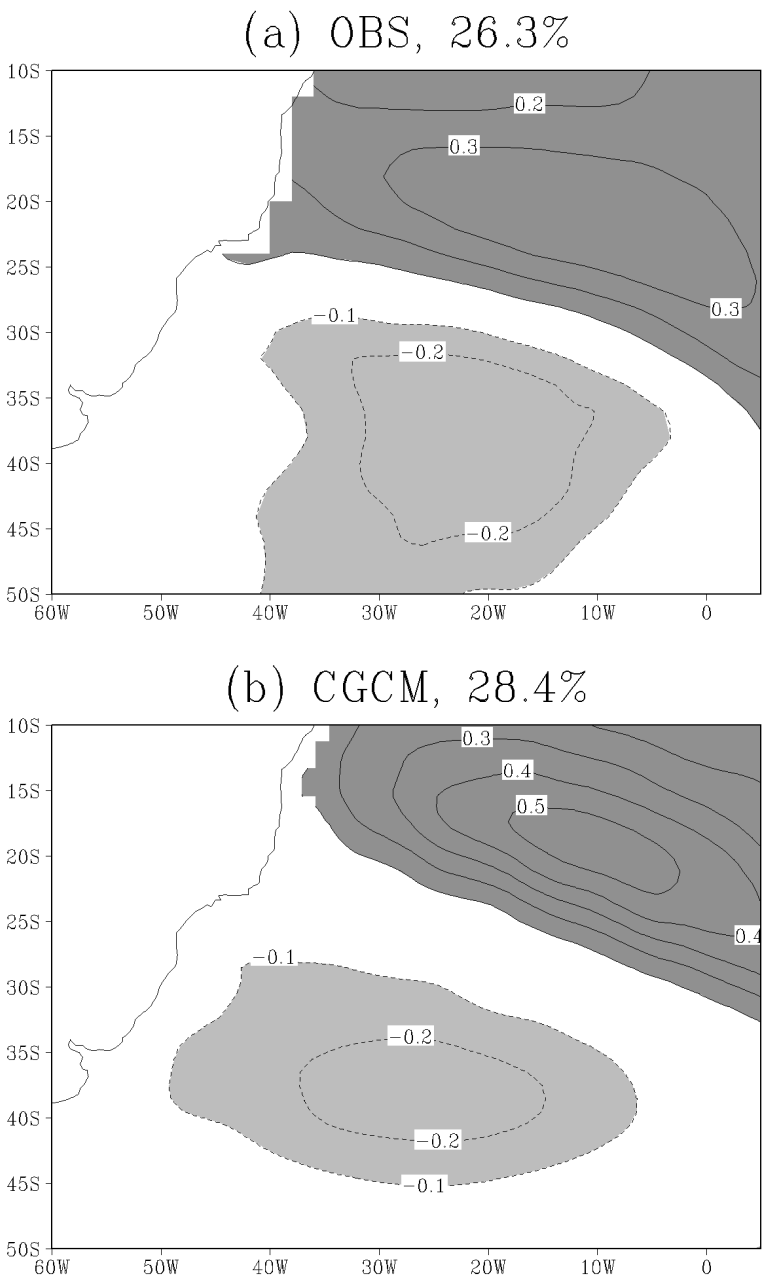

Figure 2 The spatial structures of the 1st EOF modes of the SSTA in the South Atlantic Ocean for (a) the observations for 1950-2000 and (b) the 300-yr CGCM simulation. The number on each panel gives the percentage of total variance explained by the mode. The corresponding principal components of these modes are normalized to have unit standard deviation. The contour interval is 0.1°C with zero lines omitted. Areas with loadings less than -0.1°C are lightly shaded and those larger than 0.1°C are darkly shaded.

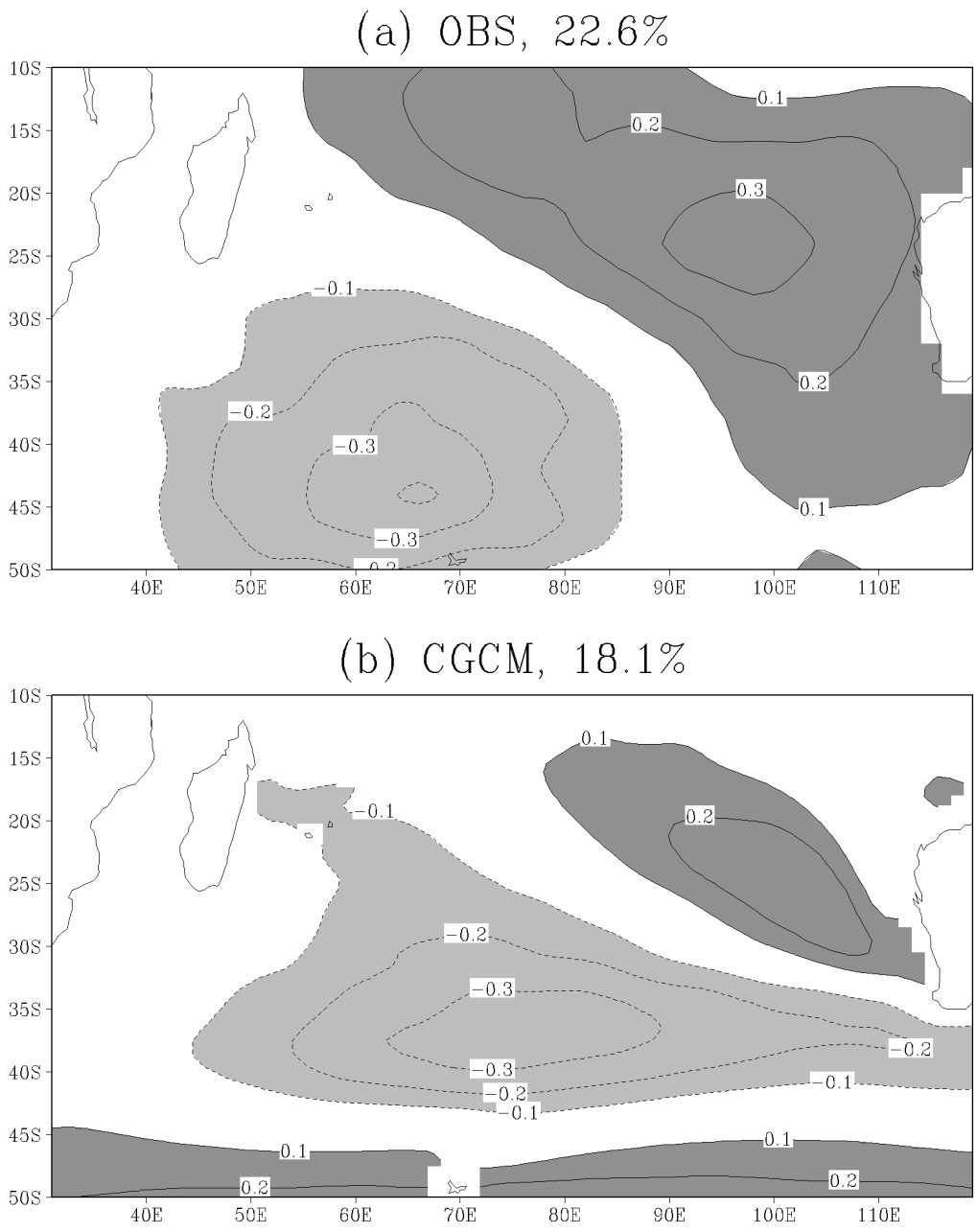

Figure 3 The spatial structures of the 1st EOF modes of the SSTA in the South Indian Ocean for (a) the observations for 1950-2000 and (b) the 300-yr CGCM simulation. The number on each panel gives the percentage of total variance explained by the mode. The corresponding principal components of these modes are normalized to have unit standard deviation. The contour interval is 0.1°C with zero lines omitted. Areas with loadings less than -0.1°C are lightly shaded and those larger than 0.1°C are darkly shaded.

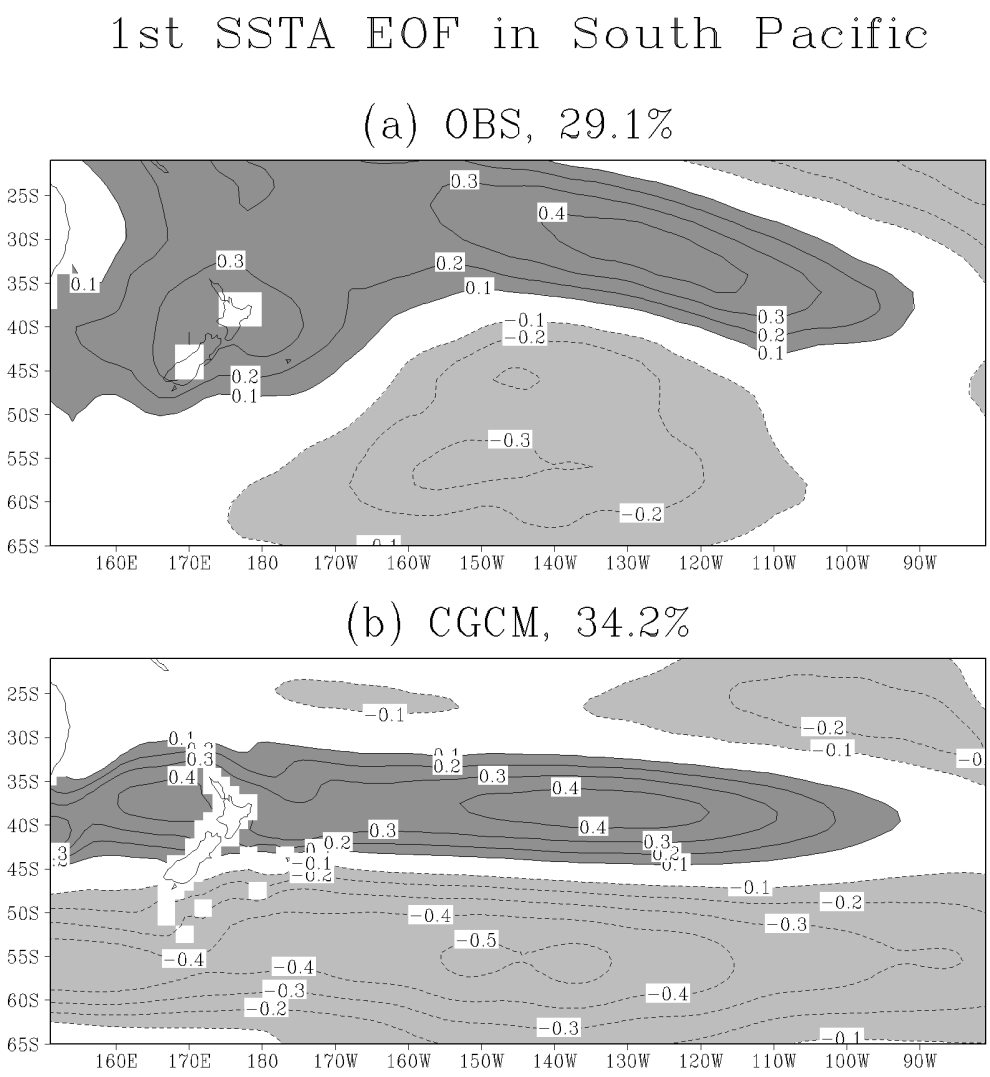

Figure 4 The spatial structures of the 1st EOF modes of the SSTA in the South Pacific Ocean for (a) the observations for 1950-2000 and (b) the 300-yr CGCM simulation. The number on each panel gives the percentage of total variance explained by the mode. The corresponding principal components of these modes are normalized to have unit standard deviation. The contour interval is 0.1ºC with zero lines omitted. Areas with loadings less than -0.1ºC are lightly shaded and those larger than 0.1ºC are darkly shaded.

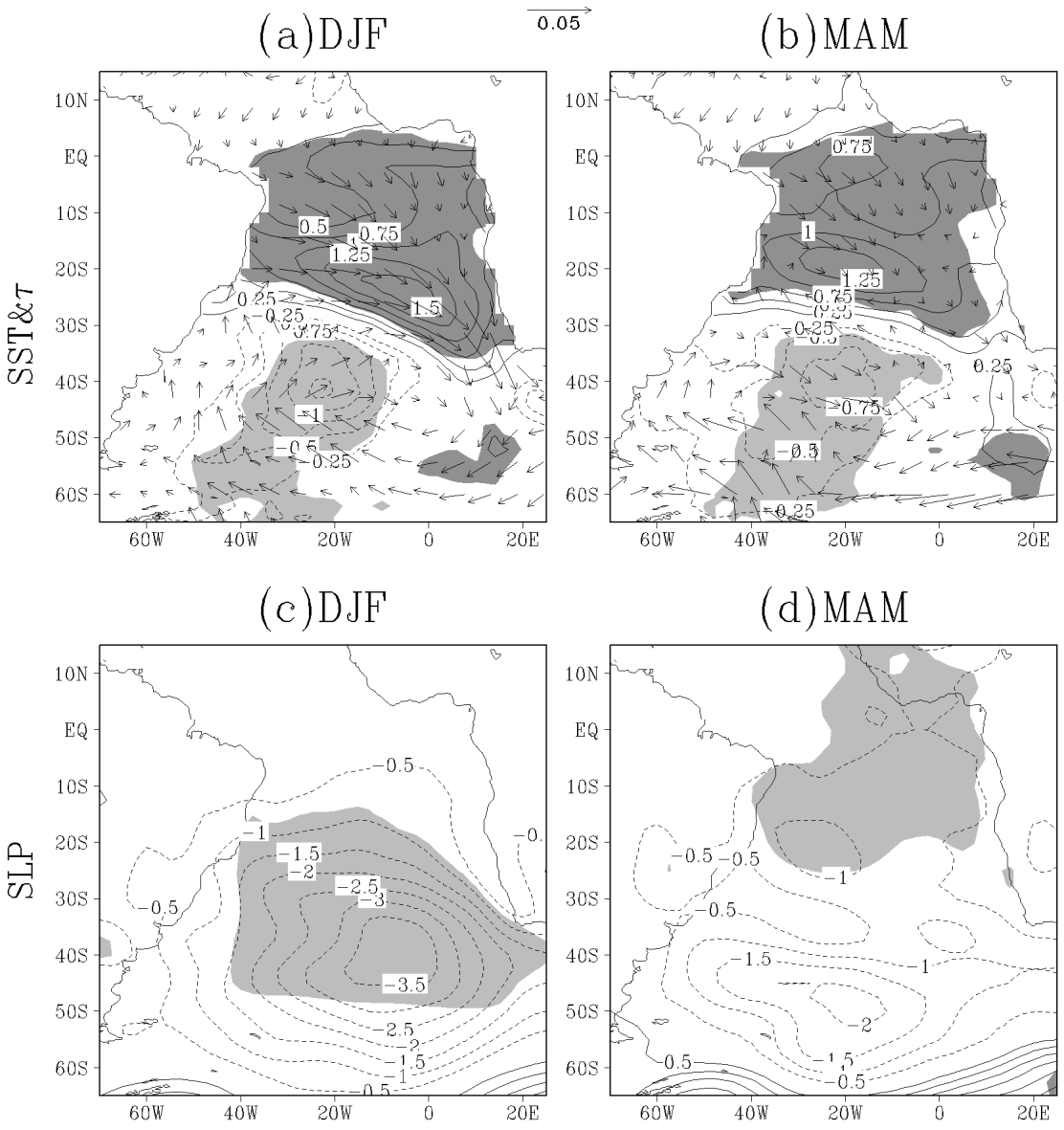

Figure 5 The observed differences between the positive and negative composite events in the South Atlantic during the evolution from austral summer (left) to fall (right). The upper panels show the SSTA (ºC) and wind stress anomalies (Nm^{-2}). The lower panels show the SLP anomalies (hPa). The contour intervals are 0.25ºC for SST and 0.5hPa for SLP. Zero contours are omitted in all panels. The length of wind vector at $0.05Nm^{-2}$ is shown in the top center of the upper panels. The shadings give the regions above the 95% significance level for SST and SLP.

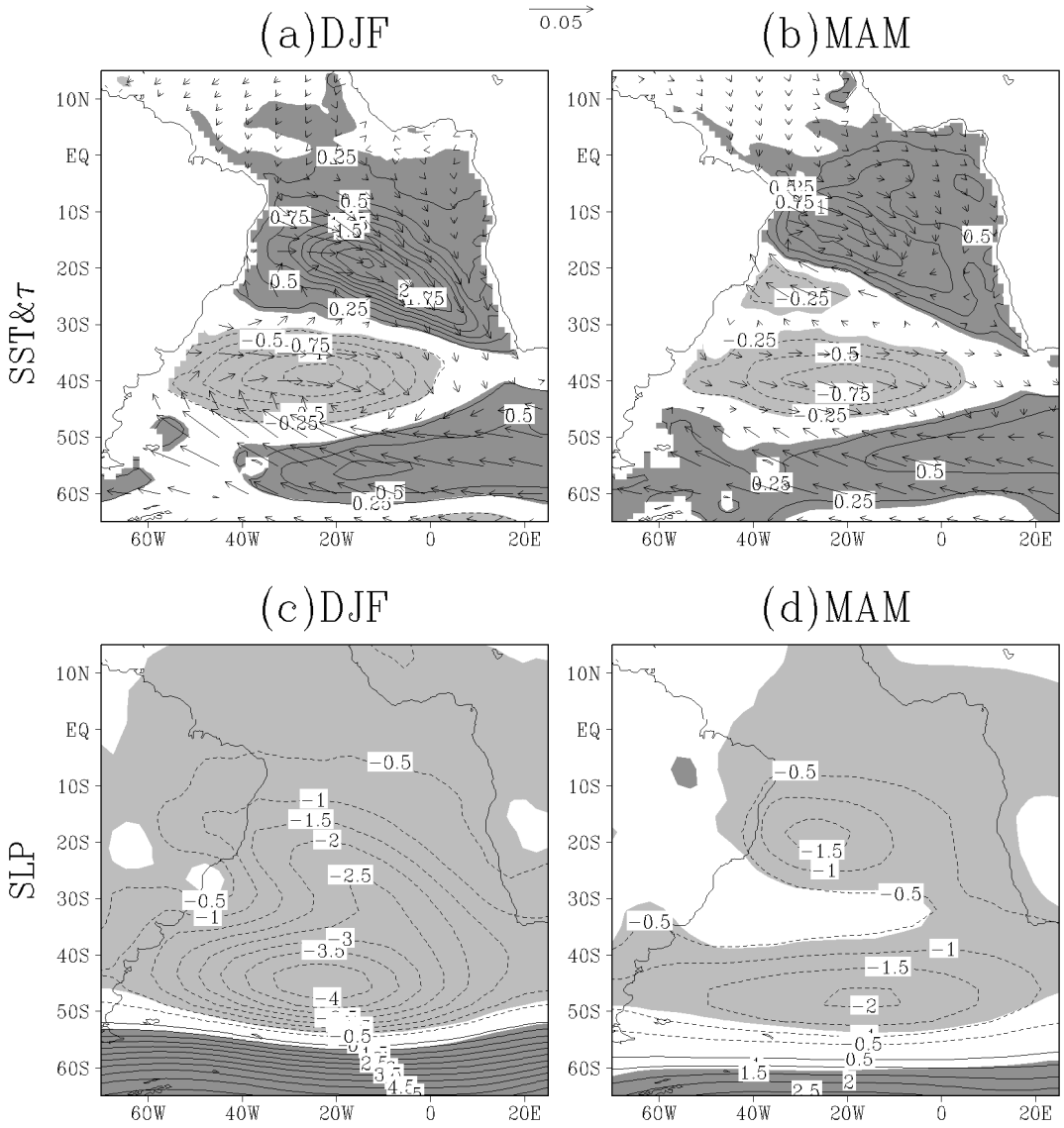

Figure 6 The CGCM differences between the positive and negative composite events in the South Atlantic during the evolution from austral summer (left) to fall (right). The upper panels show the SSTA (ºC) and wind stress anomalies (Nm^{-2}). The lower panels show the SLP anomalies (hPa). The contour intervals are 0.25ºC for SST and 0.5hPa for SLP. Zero contours are omitted in all panels. The length of wind vector at $0.05Nm^{-2}$ is shown in the top center of the upper panels. The shadings give the regions above the 95% significance level for SST and SLP.